

Michael A. Magsig^{1*}, James G. LaDue¹, Erik N. Rasmussen², and Jerry M. Straka³
¹NOAA/NWS/Warning Decision Training Branch, Norman, OK
²Rasmussen Systems LLC, Mesa, CO
³University of Oklahoma, Norman, OK

1. INTRODUCTION

In traditional photogrammetry, pixels in a photograph are mapped to space using the position of the camera and the location of known features in the photograph (Holle 1982). This can be accomplished with a time-consuming process involving taking a surveyor transit to the photograph site and precisely measuring the relative position of features in the photograph. Varying degrees of accuracy in measurements can be achieved by taking into account the characteristics of the camera such as focal length, pitch, roll, yaw, and using multiple photographs (i.e. stereo photogrammetry) from different angles (Rasmussen et al. 2003).

Photogrammetry has been used for decades in a number of different ways in severe storm research to study thunderstorms and tornadoes. Golden and Purcell (1978) used photogrammetry for tracking the motions of objects around a tornado from successive images. Wakimoto and Bringi (1988) and Wakimoto and Martner (1992) used photogrammetry to map ground-based radar data to the visual cloud. Wakimoto et al. (2003) used photogrammetry to overlay airborne Doppler radar data with tornado photos in the Verification of the Origins of Rotation in Tornadoes Experiment (VORTEX; Rasmussen et al. 1994).

For the Verifications of the Origin of Rotation in Tornadoes Experiment 2 (VORTEX2) we developed a less time consuming approach for photogrammetry using high-resolution Global Positioning Systems (GPS; see Fig. 1). We collected numerous stereo photography observations on the rear-side of supercell thunderstorms to use the photogrammetry to investigate the characteristics of the clear slot and rear-flank downdraft which are important in tornadogenesis. The data collection strategies will



Figure 1. The photogrammetry camera base station including: 1) Promark3 GPS (bottom), GPS antenna (top), Nikon D300 camera fixed to a custom-built tripod mount with digital protractors on the rear and left side of the mount to measure pitch and roll.

*Corresponding author address: Michael Magsig,
 WDTB, 120 David L. Boren Blvd, Suite 2460,
 Norman, OK 73072, email:
 Michael.A.Magsig@noaa.gov.

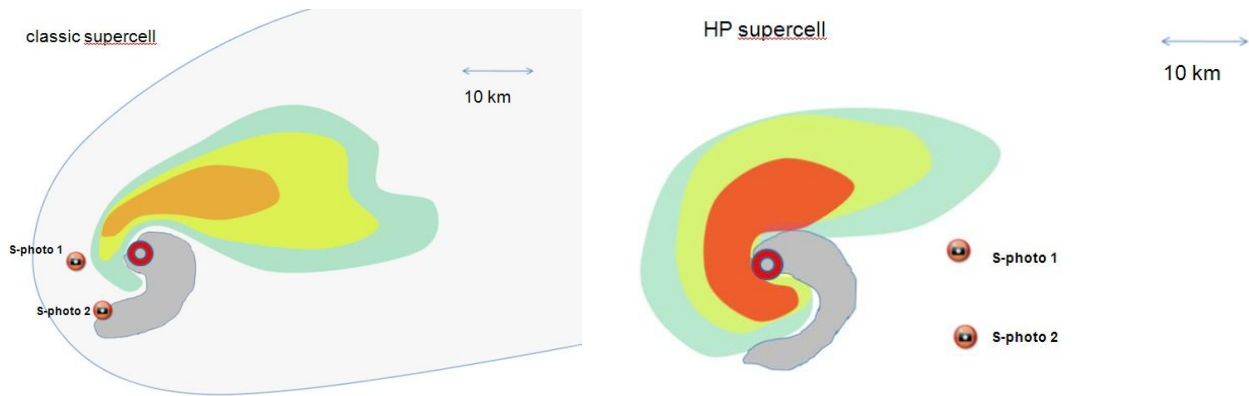


Figure 2. Ideal positioning for the two camera teams (S-photo 1 and S-photo2) to photograph the back side of a classic supercell (left) and the front side of an HP supercell (right). The dark grey shading represents low-level updraft. Colored shading represents radar reflectivity, and the circle represents center of low-level rotation.

be discussed in section 2.1, and the equipment will be discussed in section 2.2. The observations we collected in VORTEX2 will be discussed in section 2.3.

2. VORTEX2 STORM-SCALE PHOTOGRAMMETRY

2.1 Data Collection Strategies

In VORTEX2 we used two teams in separate vehicles to collect photographs of thunderstorms for stereo photogrammetry. One important restriction in data collection was that the cameras needed to be kept out of the rain for mechanical and visibility reasons. For the ideal slow moving classic supercell (Fig. 2), our strategy was to collect observations in the clear slot on the back side of the updraft to investigate the characteristics of the cloud boundary and the rear-flank downdraft. This required constant communications to ensure we were viewing the same cloud features with the appropriate geometry. Many of the storms VORTEX2 sampled did not have well-defined large long-lived clear slots with good visibility. In general many of the notches sampled were small, short lived, and difficult to anticipate and deploy on. Deployments were relatively short, and much of the time was spent positioning for the narrow window of opportunity for a good deployment.

For an HP supercell (Fig. 2), our strategy was to collect observations on the forward side of the updraft. As the storm approached close range (optimal for photogrammetry), we needed to quickly pick up the equipment to avoid the severe

weather and getting out of position for the next potential deployment.

There are many factors leading to uncertainty in stereo photogrammetry positioning estimates, including azimuth, pitch, roll, distance between the cameras (i.e. baseline length), and range to the feature being photographed. In order to have error estimates on the order of 100 m for combining with radar data, our goal was to develop a solution with 0.1 degree accuracy in azimuth, pitch, and roll. For a given azimuthal accuracy, the position uncertainty due to the simple geometry can be calculated for a wide variety of camera orientations and distances to the storm. Figure 3 illustrates the position uncertainty as a function of camera baseline and range to target assuming 0.1 degree accuracy in camera orientation. The green area in Figure 3 illustrates optimal combinations of baseline and range for our purposes. While our initial plans were to establish camera baselines of ~10km with distances to the updrafts < 10-20km, in general we found that we had to use much shorter baselines and at times longer than desired ranges to the updraft due to visibility, road network, storm speed, time for deployment, etc.

2.2 Equipment

We chose to use two Nikon D300 Digital SLR cameras due to low cost, 12MP image resolution, good performance in low light conditions, and interval shooting capability which allowed us to automatically take pictures every 5 seconds. We chose a 10-20mm wide angle lens to minimize distortion while still providing large field of views. At moderate ranges we routinely used 20mm focal

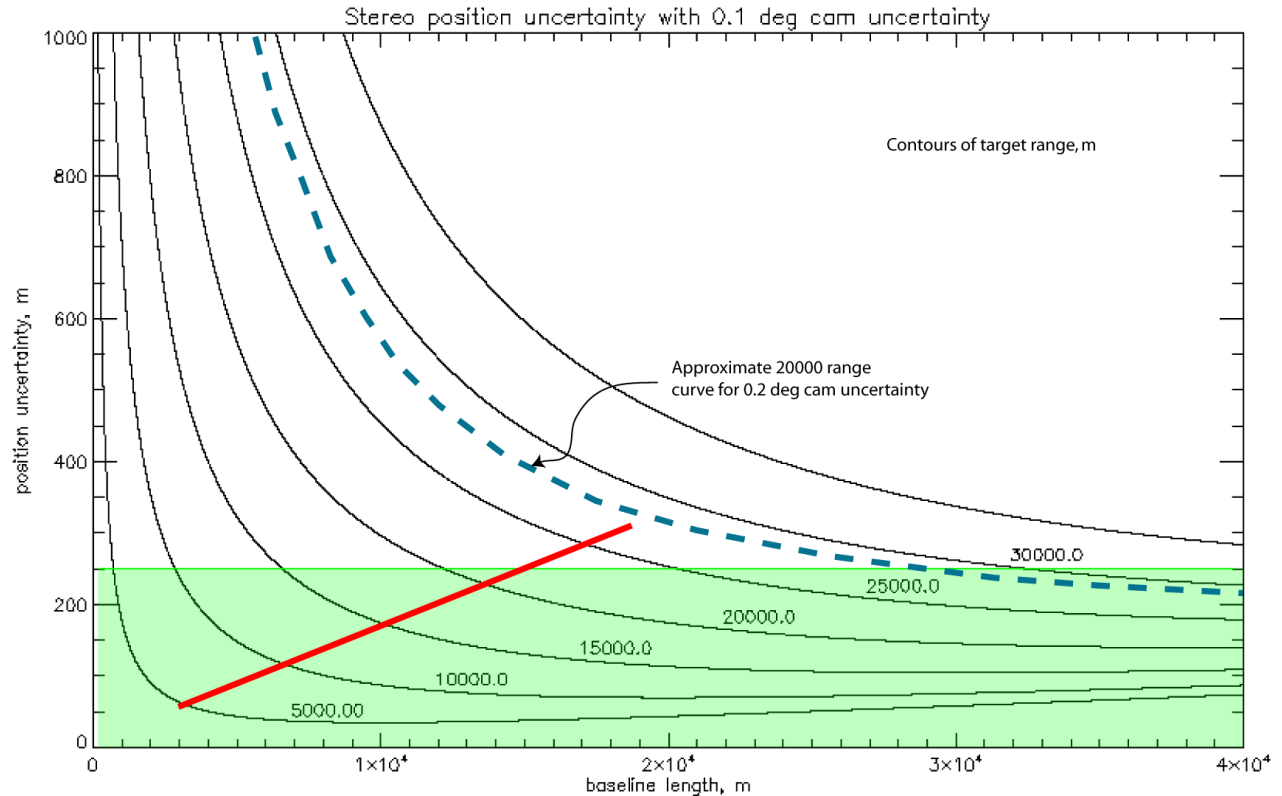


Figure 3. Position uncertainty (Y-axis) in stereo photogrammetry as a function of camera baseline length (i.e. distance between cameras) on the X-axis, range to updraft (solid lines) for a camera uncertainty of 0.1 degrees. Green areas denote desired combinations of baseline and range to updraft. The red line indicates where errors start to grow quickly with small changes in increasing range. The dashed line provides a reference for directional uncertainty of 0.2 degrees at 20km range.

length settings on both cameras to minimize distortion, and at close ranges we many times used 10mm to capture all the structure and allow for longer deployments as features were in the field of view longer. The camera automatically stored the focal lengths and time in the photo's EXIF header. Cameras were synced to atomic time to the nearest second prior to each day's first deployment.

For this experiment we needed 0.1 degree accuracy in azimuth, pitch, and roll. Traditional magnetic-based digital compasses did not provide the desired azimuthal accuracy. Discussions with survey experts led us to use standard high-resolution differential GPS technology to determine azimuth. The basic idea is to use two GPS units with high positional accuracy (cm and potentially mm at times) to compute azimuth with the camera attached to one GPS.

In our solution, one GPS antenna was mounted over the CCD sensor of the camera using a custom-built tripod mount (see Fig. 1). The mount was developed and cut precisely from a

local machine shop. The camera was fit to the mounting plate using a camera-specific mounting L bracket to ensure the camera was securely aligned with the geometry of the plate. Throughout two years of field work, there was never any wiggle in the camera connection to the plate. Thumb screws on orthogonal bars allowed for positioning the center of the antenna over the CCD sensor and keeping the antenna level. The plane of the CCD sensor location was marked on the side of the camera, and the intersection of the center of the lens with the CCD plane was used to align the antenna when the GPS was set up.

In addition to the camera "base" GPS, a second "rover" GPS was deployed on a bipod in the field of view of the camera (Fig. 4). Each GPS would take around 5-10 minutes to reach observational range where the positional estimates would support high accuracy. During this time the camera and GPS units could not be moved, or the process would need to start over. After operations were over we would post process the GPS data using Magellan's GNSS solutions



Figure 4. Front side deployment on an HP supercell on Jun 10, 2009 with camera base station (lower right) and rover GPS on yellow bipod (center). Also shown is an intermediate tripod holding a water hose used as a redundant measure of horizon. Radar reflectivity (upper left) with team positions (stars) shows where camera was located (purple star).

software. This software uses the differential GPS information between the base and rover GPS units to provide highly accurate antenna locations and the azimuth between the two GPSs. Because the antenna of the base GPS was located directly above the camera's CCD chip, the calculated azimuth is valid at the center of the antenna location of the rover in the field of view of the photo.

A SmartTool Pro 3600 digital protractor with 0.05 degree accuracy was used to determine pitch, and a SmartTool Pro 360 digital protractor with 0.1 degree accuracy was used to determine roll. These digital protractors were secured to the mount precisely aligned with the edges of the mount to be orthogonal to each other. The digital protractor documentation stated that large temperature changes (~10F) on the order of what we experience in data collection could cause errors in measurements. It also suggested that recalibration should be performed every time this happened. This was not feasible during deployments, so we enlisted a redundant check on

the pitch and roll calculations using a water level in a hose. While the camera was taking pictures, one person would align the water level in the hose at the height of the CCD chip while another person would take the other end of the 15m hose into the field of view of the camera. A water level observation was taken on each side of the field of view of the camera when pictures were being taken to establish the pixel location of the horizon. The horizon information and the image geometry were combined to determine the pitch and roll. The protractor measurements and water level measurements were compared to each other, and they were found to be in very close agreement. While the protractors were recalibrated multiple times during the experiment, the observations were remarkably consistent given the variety of environments they were exposed to. The errors in drift were rarely significant, except when first calibrated after a year of not being used. Therefore we have confidence in the accuracy of the pitch and roll measurements.

Date	Preliminary Notes on Type/Location
20090515	QLCS nw-OK
20090519	High-based multicell nw-OK
20090520	Weak supercell Alliance, NE
20090523	Small multicell Grant, NE
20090525	3 dying cells Sayre, OK
20090526	Left mover Decatur, TX
20090529	Multicells Taylor, NE
20090531	Multicells Thurman, IA
20090601	Large multicell Hebron, NE
20090604	Supercell Cheyenne, WY
20090605	Tornadic supercell WY
20090606	Supercell Mullen, NE
20090607	Tornadic supercell Oregon, MO
20090609	Nontornadic supercell DDC
20090610	QLCS-HP Hugoton, KS
20090611	Nontornadic supercell Lamar, CO
20090613	Small multicell Panhandle, TX
20100506	Elev supercell Oberlin, KS
20100512	HP supercell w-OK
20100514	Multicell Midland, TX
20100515	Supercell Artesia, NM
20100517	Supercell Artesia, NM
20100518	HP supercell Dumas, TX
20100519	HP supercell Kingfisher, OK
20100521	Supercell Goshen Co, WY
20100523	Supercell Leoti, KS
20100524	Supercell Sutherland, NE
20100525	Supercell Tribune, KS
20100526	Supercell Prospect Valley, CO
20100603	Supercell se-SD, NE
20100606	HP supercell Grant, NE
20100607	HP supercell ScottsBluff, NE
20100609	Supercell Hawk Springs, WY
20100610	Tornadic supercell Deer Trail, CO
20100611	HP supercell Genoa, CO
20100612	n-TX panhandle supercell
20100613	Toradic supercell ne-TX pan
20100614	Gustnados Tahoka, TX

Table 1. Dates of data collected with preliminary notes on storm type and location.

For the most part, the Promark3 GPS units were reliable in collecting observations. Occasionally there would be interference at certain locations or a loose connection that would prevent the GPS from finding satellites. These isolated issues were addressed as they came up, and for most days the technology supported multiple deployments. Sometimes it would take longer than 5-10 minutes to reach observational range (e.g. first deployment of the day in a new geographic area) before the units could be shut down. The

optimal windows for photogrammetry deployments on good roads with good visibility were generally short lived, and any future improvements to save minutes of time could significantly improve data collection.

2.3 Observations

Data were collected on 17 days in 2009 (May 15, 19, 20, 23, 25, 26, 29, 31, and June 1, 4, 5, 6, 7, 9, 10, 11, 13) and 21 days in 2010 (May 6, 12, 14, 15, 17, 18, 19, 21, 23, 24, 25, 26, and June 3, 6, 7, 9, 10, 11, 12, 13, 14; see Table1). The number of deployments per day typically ranged from 1-3. As noted by Magsig et al. (2006), the rear side of the updraft looks significantly different from the often photographed front side (Fig. 5). The data analyzed so far reveals a wide variety of structures on the rear side (Figures 6 and 7). We observed many types of small scale and sometimes transient clefs/notches on the back side of the updrafts, but relatively few were the large clear slots as in the classic conceptual model (and Fig 5). Research is continuing at the time of this preprint into all the datasets collected, and future work will be to combine the radar data with the photographs to identify the location of the RFD relative to the cloud boundary throughout the depth of the clear slot.

3. CONCLUSIONS

We have demonstrated a new way to collect highly accurate stereo photogrammetry using high-resolution differential GPS technology along with digital protractors and manual water levels.

Not having to survey the area with a transit greatly reduced the time required to complete the photogrammetry. While this is a big step forward from previous approaches, to adequately sample the quickly evolving features in the rear-flank downdraft, a more responsive and mobile solution would be optimal. In future research projects we recommend a mobile platform be built with multiple GPS antennas fixed to a vehicle with a camera mount. This would remove setup and take down time, and it would greatly increase the number of observations taken.

4. ACKNOWLEDGEMENTS

We would like to thank the following participants who contributed to collecting VORTEX2 photogrammetry field observations: Aaron Anderson, Ben Baranowski, Karen Braun, Veronica Davis, Stefanie Henry, Aaron Kennedy,

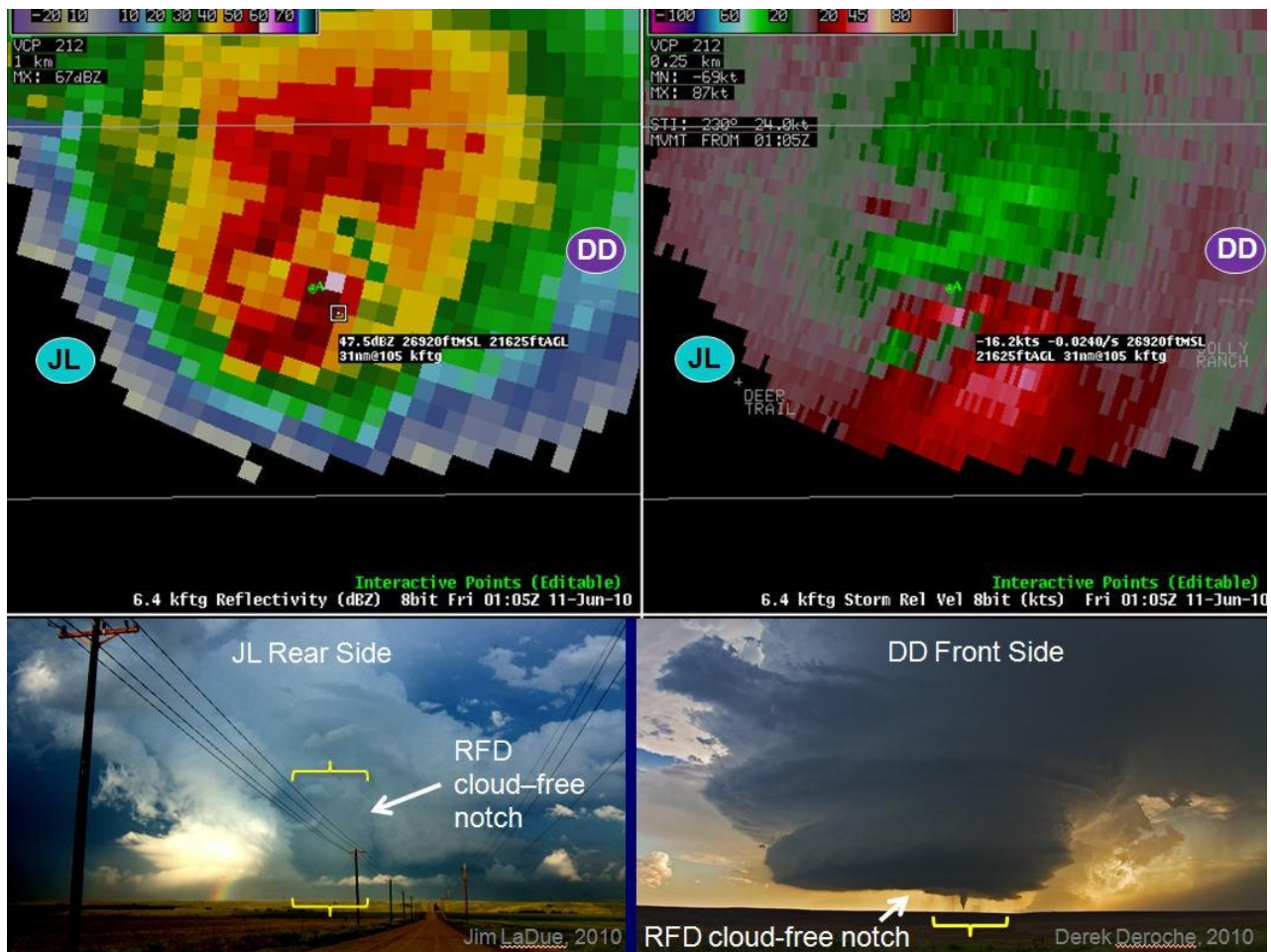


Figure 5. Radar reflectivity at 6.6 km (22 kft) AGL in upper left, storm-relative velocity at 8.6 km (22 kft) AGL in upper right, rear side photogrammetry picture from Jim LaDue (JL location annotated in top plots) in lower left and front side picture from storm chaser Derek Deroche (DD location annotated in top plots) in lower right for the June 10, 2010 Deer Trail, CO storm. Rear side updraft appearance is much different from front side.

Darrel Kingfield, Amanda Kis, Peter Laws, Stephen Martinaitis, Kiel Ortega, Clark Payne, Mikko Rauhala, Larissa Reames, Mark Sessing, Chris Spannagle, Greg Stumpf, Cynthia Van Den Broeke, and Matthew Van Den Broeke. We would also like to thank Sean Waugh and Brian Baker for assistance with retrofitting the vehicles for field observations. This research was supported by NSF ATM #0733531 and #0733539.

5. REFERENCES

- Holle, R.L., 1982: Photogrammetry of thunderstorms, *Thunderstorms: A Social and Technological Documentary*, E. Kessler, Ed., University of Oklahoma Press. 77-98.
- Magsig, M. A., J.G. LaDue, and M. Yuan, 2006, Visual Characteristics of Severe Storms, Preprints, 23rd Conf. on Severe Local Storms, St. Louis, MO, Amer. Metero. Soc., J14.2.
- Rasmussen, E.N., J.M. Straka, R. Davies-Jones, C. A. Doswell III, F. H. Carr, M. D. Eilts, and D. R. MacGorman, 1994: Verification of the Origins of Rotation in Tornadoes Experiment: VORTEX, *Bull. Amer. Met. Soc.*, **75**, 995-1006.
- _____, R. Davies-Jones, R.L. Holle, 2003: Terrestrial Photogrammetry of Weather Images Acquired in Uncontrolled Circumstances, *J. Atmo. And Oceanic Tech.* **20**, 1790--1803.
- Wakimoto, R. M. and V. N. Bringi, 1988: Dual-polarization observations of microbursts associated with intense convection: the 20 July storm during the MIST project, *Mon. Wea. Rev.*, **116**, 1521-1539.



Fig 6. Rear side of Jun 11, 2009 Lamar, CO storm at two different times and locations. Notice the large number of small clefts in the updraft towers on the lower image.



Fig 7. Rear side of Jun 9, 2009 Dodge City, KS storm (top) with lots of precip on the back side and a deep cleft on the flanking line on the right side of the image. The storm became much drier at the end of its life (bottom), and it had a well defined clear slot.

_____, and B.E. Martner, 1992: Observations of a Colorado tornado. part II: combined photogrammetric and doppler radar analysis, *Mon. Wea. Rev.*, **120**, 522-543.

_____, H. V. Murphey, D. C. Dowell, H.B. Bluestein, 2003: The Kellerville Tornado during VORTEX: Damage Survey and Doppler Radar Analysis, *Mon. Wea. Rev.*, **124**, 384-407.